

Novel mechanism of photoinduced reversible phase transitions in molecule-based magnets

Tohru Kawamoto, Yoshihiro Asai, and Shuji Abe

Electrotechnical Laboratory, Agency of Industrial Science and Technology (AIST), 1-1-4 Umezono, Tsukuba 305-8568, Japan.
(October 31, 2018)

A novel microscopic mechanism of bi-directional structural changes is proposed for the photo-induced magnetic phase transition in Co-Fe Prussian blue analogues on the basis of *ab initio* quantum chemical cluster calculations. It is shown that the local potential energies of various spin states of Co are sensitive to the number of nearest neighbor Fe vacancies. As a result, the forward and backward structural changes are most readily initiated by excitation of different local regions by different photons. This mechanism suggests an effective strategy to realize photoinduced reversible phase transitions in a general system consisting of two local components.

78.90.+t,71.35.-y,71.35.Lk,78.20.-e

Repeatable switching-on and -off of magnetization by external stimuli such as light is one of the most fascinating phenomena with potential applications in next generation's information storage and processing. A bi-directional photo-induced magnetization was first discovered in a cobalt-iron Prussian blue analogue, $K_{0.4}Co_{1.3}Fe(CN)_6 \cdot 5H_2O$ [1–3]. Illumination of visible light (500 - 700 nm) at low temperature induces a bulk magnetization (presumably, ferrimagnetism), which can be eliminated by illumination of near-IR light (~ 1300 nm). In spite of various experimental and theoretical efforts [1,2,4–8], the microscopic mechanism of the reversible magnetization is still not clear. In this Letter we report *ab initio* quantum chemical cluster calculations for the Co-Fe Prussian blue analogue, unveiling the microscopic mechanism of the bi-directional photo-induced local structural changes that trigger the phase transitions.

The crystal of a Prussian blue analogue $K_{1-2x}Co_{1+x}Fe(CN)_6$ is composed of two metallic sites located on vertices of the cubic lattice and each surrounded by six cyano moieties, as shown in Fig. 1. The *d*-orbitals of transition metals split into t_{2g} and e_g orbitals by the ligand field. In the case of $x \neq 0$, there are vacancy sites with replacement of CN by H_2O as shown in Fig. 1(b). Various fascinating phenomena including a room temperature magnet [9], electrochemically tunable magnets [10], transparent and colored magnetic thin films [11], and photo-induced magnetic dipole inversion [12] have been observed in such non-stoichiometric compounds. We will show that this non-stoichiometric aspect is essential for the reversible photo-induced magnetization.

The low spin (LS) configuration of the ground nonmagnetic state and the high spin (HS) configuration of the meta-stable magnetic state of $K_{0.4}Co_{1.3}Fe(CN)_6 \cdot 5H_2O$ are most likely $Co^{III}(d\epsilon^6, S = 0)Fe^{II}(d\epsilon^6, S = 0)$ and $Co^{II}(d\epsilon^5 d\gamma^2, S = 3/2)Fe^{III}(d\epsilon^5, S = 1/2)$, respectively [1,2]. These are depicted in Fig.2 as LS0 and HS0 states. Figure 2 schematically represents the most plausible el-

ementary processes in the cycle of the photo-induced structural change. The LH0 and HS0 states are converted to the intermediate states LS1 and HS1, respectively, by photo-induced charge transfer (CT) between iron and cobalt atoms, and then to the final states HS0 and LS0 by intersystem crossing due to spin-orbit coupling at cobalt sites. The major structural difference between the LS and HS states lies in the Co-N bond length $d(Co-N)$, which is longer by about 0.2\AA in HS than in LS [13]. This implies that the transition between LS and HS states requires a volume change, which may be a major origin of a large energy barrier between them, as in the case of a spin-crossover complex [14,15].

Based on these observations, we adopt a cluster model consisting of a cobalt ion and surrounding cyano ligands with a variable bond length between Co and N. Previously we carried out first-principles band structure calculations [7]. It was found that the relevant *d*-bands have quite narrow widths compared with the level spacings, implying that the *d*-electrons are fairly localized with weak charge transfer character in this material. This allows us to use the cluster approach in the present paper. We have checked that cluster calculations produce results that are consistent with band structure calculations [7].

To take into account the partial substitution of ligands by water molecules, we consider the following three clusters with various numbers N_W of H_2O substitutions: (a) $Co(NC)_6$ ($N_W=0$), (b) $Co(NC)_5 \cdot H_2O$ ($N_W=1$), and (c) $Co(NC)_4 \cdot 2H_2O$ ($N_W=2$). Bond lengths other than Co-N are fixed at observed values, e.g., $d(C-N)=1.12\text{\AA}$ [13]. The potential energies of the four relevant states shown in Fig.2 are calculated for these clusters by using a quantum chemical *ab-initio* calculation program with the MIDI basis function set [16,17]. The multi-configuration self-consistent field (MCSCF) method is used with an active space limited to five orbitals mainly composed of Co-*d* atomic orbitals. The spin orbit coupling was not included to obtain the energy curve for each spin state.

As for the treatment of surrounding atoms outside the

cluster, we use a lattice of atomic point charges evaluated from our previous band calculation [7]. The Fe-C bond length is fixed at the observed value 1.91Å [13]. The environment lattice contains one or two iron vacancies situated just outside the water molecules of the clusters (b) and (c). The energies of the four states are calculated for each value of $d(\text{Co-N})$ common to all the Co-N bonds in the cluster as well as in the environmental lattice. This choice diminishes the interfacial strain energy due to local volume change, being a suitable way to extract the tendency of the local cluster. It should be noted that the real relaxation dynamics is determined not only by the cluster potentials but also by (mainly elastic) interactions between clusters.

Since each Fe has full six coordination of CN with the fixed Fe-C distance, we assume that the energy difference between the two states $\text{Fe}^{\text{II}}(d\varepsilon^6, S = 0)$ and $\text{Fe}^{\text{III}}(d\varepsilon^5, S = 1/2)$ is a constant Δ irrespective of Co states. Then the energy difference between the LS0 and HS0 states, for example, of a Co-Fe pair is written in an additive form: $\Delta E_{\text{LS0-HS0}} = E[\text{Co}^{\text{III}}(d\varepsilon^6, S = 0)] - E[\text{Co}^{\text{II}}(d\varepsilon^5 d\gamma^2, S = 3/2)] - \Delta$. We have checked the appropriateness of this approximation by a supplementary calculation for a two-metal cluster $\text{Co}(\text{NC})_5\text{-(NC)-Fe}(\text{CN})_5$. In the following we use $\Delta=0.4\text{eV}$. This choice ensures that the ground state is in LS state at $x=0.3$ [1] and in HS state at $x=0.5$ [18] as observed experimentally.

Figure 3 shows calculated cluster potentials as functions of $d(\text{Co-N})$ for $N_{\text{W}} = 0$ and 1. We see that the energies of the charge-transferred states (LS1 and HS0) are lowered in the cluster of $N_{\text{W}} = 1$ compared with the case of $N_{\text{W}} = 0$. They become further stabilized in the cluster of $N_{\text{W}} = 2$ (not shown here). This implies that the ligand substitution enhances the electron affinity of Co. On the other hand, the energy differences between different spin states (between LS0 and HS1 and between HS0 and LS1) are rather insensitive to N_{W} , indicating that the ligand substitution does not affect the Hund coupling very much. From the calculated cluster potentials we obtain the Frank-Condon excitation energies of the CT excitations (LS0→LS1 and HS0→HS1). The results are summarized in Table I together with the observed main absorption peaks and the excitation energies responsible for the structural change. The calculated excitation energy ~ 2.3 eV of LS0→LH1 in $\text{Co}(N_{\text{W}}=1)$ reasonably corresponds to the observed absorption energy 2.4 eV inducing the magnetization. This implies that the photoinduced LS→HS transition is triggered by CT excitation mainly between a Co atom with $N_{\text{W}}=1$ and a nearby Fe atom. Note that the largest fraction (37%) of Co is in the configuration of $N_{\text{W}}=1$ in $\text{K}_{0.4}\text{Co}_{1.3}\text{Fe}(\text{CN})_6$, if iron vacancies are randomly distributed in the crystal. The Co atoms with $N_{\text{W}}=0$ (21% fraction) are disadvantageous for this process because of the large energy difference between the metastable HS0 state and the stable LS0 state with a small potential barrier for HS0, as one can see in Fig. 3(a).

In the case of the reverse (HS→LS) transition, the ex-

perimental photon energy (0.9 eV) required for demagnetization is much lower than the energy of the observed broad absorption around 2.3 eV. The latter may correspond to the calculated CT excitations at ~ 1.4 eV in $\text{Co}(N_{\text{W}}=1)$ and at ~ 2.6 eV in $\text{Co}(N_{\text{W}}=2)$, whereas the former is assigned to the excitation energy of $\text{Co}(N_{\text{W}}=0)$ at ~ 0.8 eV. This implies that the HS→LS transition is triggered mainly by the excitation of Co atoms with $N_{\text{W}}=0$, in contrast to the forward transition. This is reasonable, because the final LS0 state is much lower in energy than the initial HS0 state in the case of $N_{\text{W}}=0$ shown in Fig. 3(a).

The suggested main relaxation paths in the reversible transitions are indicated by arrows in Fig. 3. The path for the LS→HS transition is shown in the case of $N_{\text{W}}=1$, and the path for the reverse transition is indicated in the case of $N_{\text{W}}=0$. The Frank-Condon photo-excitations induce CT between cobalt and iron cations. The intermediate excited states are subsequently transformed into local meta-stable states via intersystem crossing due to the spin-orbit interaction at cobalt site. The magnitude of the spin orbit coupling has been estimated as about 10 meV [19]. This is much smaller than that of the typical energy scale of the potential diagram in Fig. 3. On the other hand, it corresponds to a time scale less than 1ps, which is much faster than the time scale of the photoinduced phase transition. Experimentally, intersystem crossing has been observed to occur with large probabilities in similar cobalt complexes [20].

The most important conclusion from our results is that the forward and the backward changes are initiated from spatially different local regions in the crystal. The difference lies in the cluster potential for Co electrons due to the difference in the number of ligand substitutions: $N_{\text{W}}=0$ or 1. The large concentration of Fe vacancies in this crystal, which might otherwise be thought to be a shortcoming of this material, is an essential prerequisite for the reversible transformations. The present model also implies that the photoinduced change must be a cooperative phenomenon [15,21–23], because the structural change of the entire crystal is induced by excitations in a fraction of the crystal. To confirm our model, a systematic experimental study with varying x in $\text{K}_{1-2x}\text{Co}_{1+x}\text{Fe}(\text{CN})_6$ is desired especially. For instance, the oscillator strength of the 3.9eV absorption peak in the LS state will be much more enhanced for smaller x because of an increased fraction of $\text{Co}(N_{\text{W}}=0)$.

Based on the present results, we are able to speculate how the initial relaxation process leads to the phase transition in the macroscopic scale. A local relaxed CT state (exciton) after the primary process is still in an excited state with a finite life time in the crystal, because it involves a strain energy due to lattice mismatch or frustration. The strain energy is released when the surrounding lattice undergoes a global change as an integration of all the local changes. There should be a critical concentration, R_{C} , of relaxed excitons, above which the fraction of the new phase increases drastically in the

crystal. Such behavior was observed in a similar photo-induced phase transition of a spin-crossover complex [15]. The exciton concentration R satisfies $P^{\text{PI}}(1 - R) = R/\tau$ in the stationary condition, where P^{PI} and τ represents the creation rate and the lifetime of exciton, respectively. The critical excitation rate P_C^{PI} is then expressed as $P_C^{\text{PI}} = R_C/[\tau(1 - R_C)]$. Therefore, the phase transition occurs more easily with a smaller excitation light intensity for a longer exciton lifetime. In the present system, the long life time of the relaxed exciton is guaranteed by its local stability as shown in Fig. 3.

The local mechanism discussed here indicates a general strategy to realize a reversible photoinduced phase transition by the use of a mixed crystal of a and b molecules. (Here a ‘molecule’ means just a structural unit in a wide sense.) Suppose both the a and b molecules are bistable between the two types of state A and B, but they are different in that the a molecule prefers the A-type state and the b molecule prefers the B-type state. (In the Prussian blue analogues the clusters with $N_W=1$ and 0 play the roles of the a and b molecules.) In the A phase of the crystal where all the molecules are in the A-type states, the b molecules are metastable locally. By selectively exciting b molecules by light, their states are readily changed to the locally stable B-type states, triggering the phase transition of the entire crystal to the B phase where all the molecules are in the B-type states. In the B phase, the story is the same with the interchanged roles of the a and the b molecules: Photo-excitation of locally metastable a molecules triggers the phase transition to the A phase.

In summary, our ab initio calculations have elucidated that the photoinduced forward and backward phase transitions are initiated by excitation of different local regions by different photons in Prussian blue analogues. Especially, the existence of a large concentration of vacancies, which might be thought as a shortcoming of this material, turned out to be essential for the bidirectional phase transition. We have also proposed that this mechanism can be generalized as an effective strategy to design a new material for bidirectional photoinduced switching.

The authors acknowledge Prof. K. Hashimoto at Tokyo University and Dr. O. Sato at Kanagawa Academy of Science and Technology for useful discussions. One of the authors (Y.A.) appreciates Prof. T. Iyoda at Tokyo Metropolitan University for communications in the initial stage of our study. Computations have been done partly using the facilities of AIST Tsukuba Advanced Computing Center.

- [3] M. Verdager, *Science* **272**, 698 (1996).
- [4] A. Goujon, O. Roubeau, F. Varret, A. Dolbecq, A. Bleuzen, and M. Verdager, *Eur. Phys. J. B* **14**, 115 (2000).
- [5] D. A. Pejaković, J. L. Manson, J. S. Miller, and A. J. Epstein, *Phys. Rev. Lett.* **85**, 1994 (2000).
- [6] K. Yoshizawa, F. Mohri, G. Nuspl, and T. Yamabe, *J. Phys. Chem. B* **102**, 5432 (1998).
- [7] T. Kawamoto, Y. Asai, and S. Abe, *Phys. Rev. B* **60**, 12990 (1999).
- [8] M. Nishino, K. Yamaguchi, and S. Miyashita, *Phys. Rev. B* **58**, 9303 (1998).
- [9] S. Ferlay, T. Mallah, R. Ouahès, P. Veillet, and M. Verdager, *Nature* **378**, 701 (1995).
- [10] O. Sato, T. Iyoda, A. Fujishima, and K. Hashimoto, *Science* **271**, 49 (1996).
- [11] S. Ohkoshi, A. Fujishima, and K. Hashimoto, *J. Am. Chem. Soc.* **120**, 5349.
- [12] S. Ohkoshi and K. Hashimoto, *J. Am. Chem. Soc.* **121**, 10591 (1999).
- [13] T. Yokoyama, T. Ohta, O. Sato, and K. Hashimoto, *Phys. Rev. B* **58**, 8257 (1998).
- [14] S. Decurtins, P. Gütllich, C.P. Kohler, H. Spiering, and A. Hauser, *Chem. Phys. Lett.* **105**, 1 (1984).
- [15] Y. Ogawa, S. Koshihara, Koshino. K., T. Ogawa, C. Urano, and H. Takagi, *Phys. Rev. Lett.* **84**, 3181 (2000).
- [16] M.W. Schmidt, K.K. Baldrige, J.A. Boatz, S.T. Elbert, M.S. Gordon, J.H. Jensen, S.Matsunaga Koseki, N. Nguyen, K.A. Su, S. Windus, T.L. Dupuis, M. Montgomery, and Jr. J.A., *J. Comput. Chem.* **14**, 1347 (1993).
- [17] *Gaussian basis set for molecular calculations*, edited by S. Huzinaga (Elsevier, Amsterdam, 1984).
- [18] S. Juszczyk, C. Johansson, M. Hanson, A. Ratuszna, and G. Malecki, *J. Phys., Condens. Matter.* **6**, 5697 (1994).
- [19] *Introduction to LIGAND FIELDS*, edited by B. N. Figgis (Interscience Publishers, New York, London, Sydney, 1966).
- [20] J. K. McCusker, K. N. Walda, D. Magde, and N. Hendrickson, *Inorg. Chem.* **32**, 394 (1993).
- [21] S. Koshihara, Y. Tokura, K. Takeda, and T. Koda, *Phys. Rev. Lett.* **68**, 1148 (1992).
- [22] S. Koshihara, Y. Takahashi, H. Sakai, Y. Tokura, and T. Luty, *J. Phys. Chem. B* **103**, 2592 (1999).
- [23] Z. Yu, Y.F. Hsia, X.Z. You, H. Spiering, and P. Gütllich, *J. Mater. Sci.* **32**, 6579 (1997).

TABLE I. Frank-Condon excitation energies of the LS and HS states evaluated from the cluster potentials (as shown in Fig. 3) for various N_W , compared with experiments of the absorption peak energies (underlined) and the excitation energies of the phase transitions (in bold).

-
- [1] O. Sato, Y. Einaga, T. Iyoda, A. Fujishima, and K. Hashimoto, *J. Electrochem. Soc.* **144**, L11 (1997).
 - [2] O. Sato, T. Iyoda, A. Fujishima, and K. Hashimoto, *Science* **272**, 704 (1996).

		Excitation Energy(eV)	
Theory		LS0→LS1	HS0→HS1
	$N_w=0$	3.9	0.8
	=1	<u>2.3</u>	<u>1.4</u>
	=2	0.7	<u>2.6</u>
Experiment			
	Absorption peak	<u>2.4</u>	<u>2.3</u>
	Photo-induced change	2.4	0.9

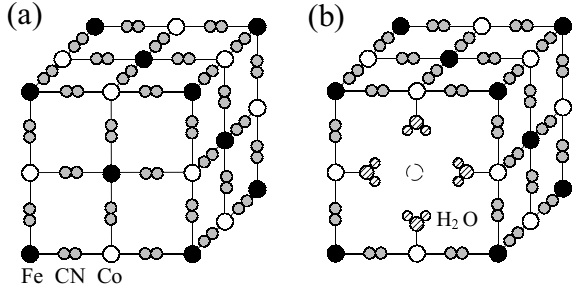


FIG. 1. Crystal structure of $K_{1-2x}Co_{1+x}Fe(CN)_6$: (a) $x = 0$; (b) $x \neq 0$. Black, white, and gray circles denote Fe, Co and CN, respectively. In (b), there is an vacancy at an iron site surrounded by six water molecules substituting cyano anions.

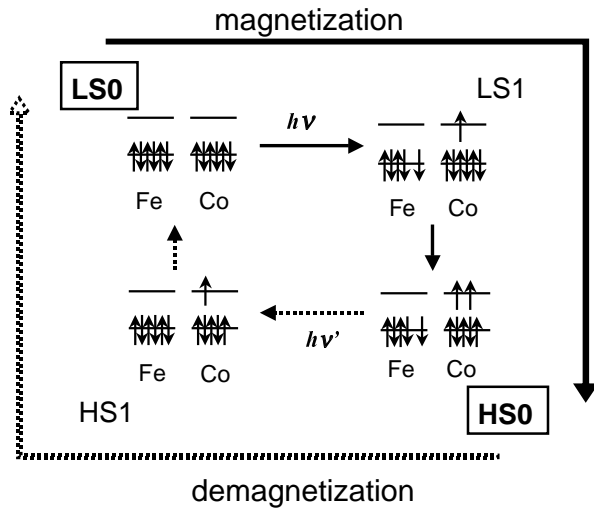


FIG. 2. Schematic local spin configurations of a Co-Fe pair. LS0, LS1, HS0, and HS1 represent the non-magnetic ground state, the paramagnetic excited state, the magnetic meta-stable state, and the magnetic excited state, respectively. The magnetization $LS0 \rightarrow HS0$ occurs through charge transfer excitation to LS1 by photon $h\nu$ and subsequent intersystem crossing (I.C.), whereas the demagnetization $HS0 \rightarrow LS0$ occurs similarly via HS1.

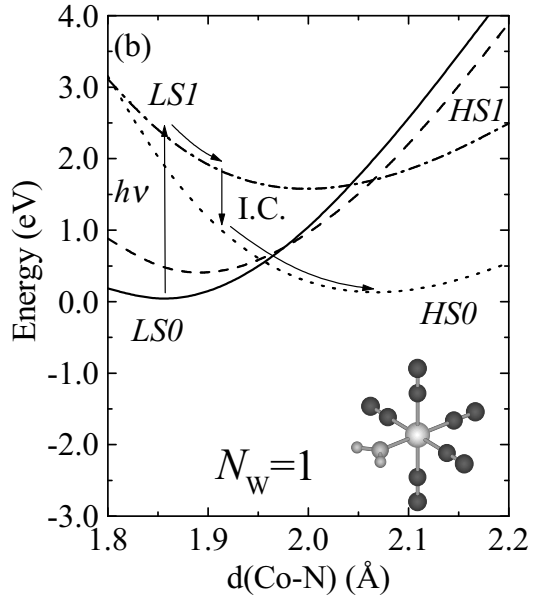
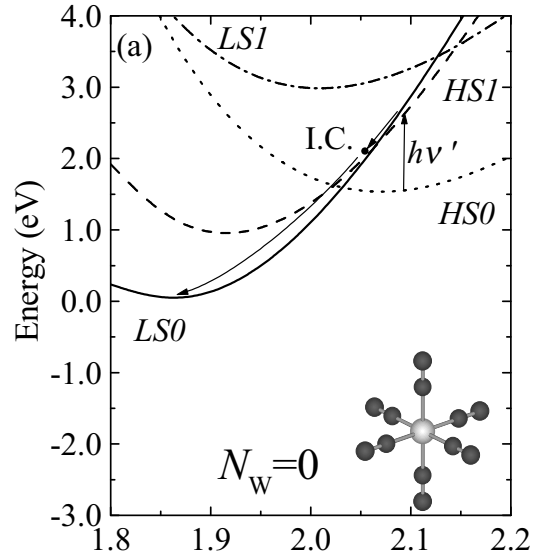


FIG. 3. Calculated potentials of the cobalt-centered clusters with (a) $N_W=0$ and (b) $N_W=1$. The LS0, LS1, HS0, HS1 states are shown by solid, broken-dotted, dotted, and broken lines, respectively. Possible primary relaxation paths for the $LS0 \rightarrow HS0$ and $HS0 \rightarrow LS0$ transitions are schematically indicated by arrows in (b) and (a), respectively (see text).